2868 *Chem. Mater.* **2009,** *21,* 2868–2874
DOI:10.1021/cm900613d

CHEMISTRY OF MATERIALS
Article

One-Pot Synthesis of Carbon-Coated SnO_2 Nanocolloids with Improved Reversible Lithium Storage Properties

Xiong Wen Lou,*[,†,‡] Jun Song Chen,[‡] Peng Chen,[‡] and Lynden A. Archer*[,†]

[†]*School of Chemical and Biomolecular Engineering, Cornell University, Ithaca, New York 14853-5201, and* [‡]*School of Chemical and Biomedical Engineering, Nanyang Technological University, 70 Nanyang Avenue, Singapore 637457*

Received March 3, 2009. Revised Manuscript Received April 17, 2009

We report a simple glucose-mediated hydrothermal method for gram-scale synthesis of nearly monodisperse hybrid SnO_2 nanoparticles. Glucose is found to play the dual role of facilitating rapid precipitation of polycrystalline SnO_2 nanocolloids and in creating a uniform, glucose-derived, carbon-rich polysaccharide (GCP) coating on the SnO_2 nanocores. The thickness of the GCP coating can be facilely manipulated by varying glucose concentration in the synthesis medium. Carbon-coated SnO_2 nanocolloids obtained after carbonization of the GCP coating exhibit significantly enhanced cycling performance for lithium storage. Specifically, we find that a capacity of ca. 440 mA h/g can be obtained after more than 100 charge/discharge cycles at a current density of 300 mA/g in hybrid SnO_2-carbon electrodes containing as much as 1/3 of their mass in the low-activity carbon shell. By reducing the SnO_2-carbon particles with H_2, we demonstrate a simple route to carbon-coated Sn nanospheres. Lithium storage properties of the latter materials are also reported. Our results suggest that large initial irreversible losses in these materials are caused not only by the initial, presumably irreversible, reduction of SnO_2 as generally perceived in the field, but also by the formation of the solid electrolyte interface (SEI).

Introduction

As a wide band gap n-type semiconductor, SnO_2 is of great importance in a growing range of technological applications, including gas sensing and lithium-ion battery anodes.[1−3] Prompted by these interests, numerous types of SnO_2 nanostructures, such as nanobelts/wires/rods, have been synthesized by a variety of approaches.[4−9] As an example, we recently reported both template-free and templating strategies for preparing high-quality SnO_2 hollow nanostructures.[10−12]

Although SnO_2 nanoparticles (ca. 10 nm in diameter) are available from a variety of commercial sources, scalable methods for synthesizing SnO_2 nanospheres of uniform size and narrow size distribution are surprisingly rare.[13,14] Previously, SnO_2 particles with mean diameters around 50 nm have been prepared by forced hydrolysis of a 3 mM $SnCl_4$ solution under strong acidic conditions.[15] These particles are composed of tiny elongated subunits, leading to a poorly defined spherical shape with rough surfaces. Despite its versatility,[16] the forced hydrolysis method usually requires a low precursor concentration, and it is also criticized for extremely low product yield.

Nanostructured tin-based materials have attracted enormous research interest as high-capacity anode materials for next-generation lithium-ion batteries.[3,8,11,17−22] When SnO_2 is used as the active component in the LIB anode, the electrochemical reaction at the anode is comprised of irreversible and reversible steps: $SnO_2 + 4Li^+ + 4e^- \rightarrow Sn + 2Li_2O$ (1); $Sn + xLi^+ + xe^- \leftrightarrow Li_xSn$

*Corresponding author. E-mail: laa25@cornell.edu (L.A.A.); xwlou@ntu.edu.sg (X.W.L.).

(1) Lou, X. W.; Archer, L. A.; Yang, Z. C. *Adv. Mater.* **2008**, *20*, 3987.
(2) Law, M.; Kind, H.; Messer, B.; Kim, F.; Yang, P. D. *Angew. Chem., Int. Ed.* **2002**, *41*, 2405.
(3) Park, M. S.; Wang, G. X.; Kang, Y. M.; Wexler, D.; Dou, S. X.; Liu, H. K. *Angew. Chem., Int. Ed.* **2007**, *46*, 750.
(4) Pan, Z. W.; Dai, Z. R.; Wang, Z. L. *Science* **2001**, *291*, 1947.
(5) Yang, H. G.; Zeng, H. C. *Angew. Chem., Int. Ed.* **2004**, *43*, 5930.
(6) Liu, Y.; Dong, H.; Liu, M. L. *Adv. Mater.* **2004**, *16*, 353.
(7) Miao, Z. J.; Wu, Y. Y.; Zhang, X. R.; Liu, Z. M.; Han, B. X.; Ding, K. L.; An, G. M. *J. Mater. Chem.* **2007**, *17*, 1791.
(8) Kim, H.; Cho, J. *J. Mater. Chem.* **2008**, *18*, 771.
(9) Zhao, Q. R.; Xie, Y.; Dong, T.; Zhang, Z. G. *J. Phys. Chem. C* **2007**, *111*, 11598.
(10) Lou, X. W.; Yuan, C.; Archer, L. A. *Small* **2007**, *3*, 261.
(11) Lou, X. W.; Wang, Y.; Yuan, C.; Lee, J. Y.; Archer, L. A. *Adv. Mater.* **2006**, *18*, 2325.
(12) Lou, X. W.; Yuan, C.; Archer, L. A. *Adv. Mater.* **2007**, *19*, 3328.
(13) Jeong, U.; Wang, Y. L.; Ibisate, M.; Xia, Y. N. *Adv. Funct. Mater.* **2005**, *15*, 1907.
(14) Deng, Z. T.; Peng, B.; Chen, D.; Tang, F. Q.; Muscat, A. J. *Langmuir* **2008**, *24*, 11089.
(15) Ocana, M.; Matijevic, E. *J. Mater. Res.* **1990**, *5*, 1083.
(16) Matijevic, E. *Chem. Mater.* **1993**, *5*, 412.
(17) Idota, Y.; Kubota, T.; Matsufuji, A.; Maekawa, Y.; Miyasaka, T. *Science* **1997**, *276*, 1395.
(18) Han, S. J.; Jang, B. C.; Kim, T.; Oh, S. M.; Hyeon, T. *Adv. Funct. Mater.* **2005**, *15*, 1845.
(19) Kim, D. W.; Hwang, I. S.; Kwon, S. J.; Kang, H. Y.; Park, K. S.; Choi, Y. J.; Choi, K. J.; Park, J. G. *Nano Lett.* **2007**, *7*, 3041.
(20) Zhang, W. M.; Hu, J. S.; Guo, Y. G.; Zheng, S. F.; Zhong, L. S.; Song, W. G.; Wan, L. J. *Adv. Mater.* **2008**, *20*, 1160.
(21) Yang, H. X.; Qian, J. F.; Chen, Z. X.; Ai, X. P.; Cao, Y. L. *J. Phys. Chem. C* **2007**, *111*, 14067.
(22) Cui, G. L.; Hu, Y. S.; Zhi, L. J.; Wu, D. Q.; Lieberwirth, I.; Maier, J.; Mullen, K. *Small* **2007**, *3*, 2066.

 Published on Web 05/29/2009

($0 \leq x \leq 4.4$) (2).[23,24] On the basis of the reversible reaction (2), the theoretical lithium storage capacity of SnO_2 can be calculated to be approximately 790 mA h/g, which is more than a factor of 2 greater than that of widely used graphite (372 mA h/g). Widespread use of these higher-capacity anode materials are, nonetheless, still largely hampered by two major issues: large initial irreversible loss and poor capacity retention over extended cycling, which conspire to make graphite the material of choice in most commercial rechargeable lithium batteries. The large initial irreversible loss of capacity is often ascribed to the irreversible reaction (1), whereas the poor capacity retention found in SnO_2 and other oxides has been widely speculated to arise from the large volume changes in the electrode materials created by Li insertion and extraction (the volume change is more than 200% when Sn alloys with Li to form $Li_{4.4}Sn$).[25] Such large, cyclic volume changes are expected to promote fatigue failure of functional particles within the active material, ultimately leading to their disintegration (pulverization), and thereby, loss of electrical connectivity with neighboring particles.

Although there is no well-established method to overcome the pulverization problem, it has been suggested that carbon coating may be an effective way to improve the cycling performance of noncarbonaceous anode materials for next-generation lithium-ion batteries, and good preliminary evidence has been demonstrated.[26−29] For example, we recently reported multistep synthesis of SnO_2@carbon hollow spheres by coating of presynthesized SnO_2 hollow spheres with glucose-derived carbon-rich polysaccharide (GCP) under hydrothermal conditions followed by carbonization.[29,30] This carbon coating strategy, like the active/inactive concept,[31] is a compromise between capacity and cycle life because carbon material is often of low activity. It is hypothesized that the carbon shell plays an important role as structural buffering layer to mitigate the mechanical stress caused by large volume change. From this point of view, carbon-coated SnO_2 nanocolloids should be desirable for reversible lithium storage. This motivation has led us to develop a simple one-pot synthesis of SnO_2@carbon composite nanostructures.

Herein, we report a simple green-chemical method for large-scale synthesis of nearly monodisperse SnO_2 hybrid particles coated selectively with/without carbon. The procedure utilizes widely available stannates and glucose as precursors. Glucose not only mediates the rapid precipitation of colloidal SnO_2 particles but also serves as a carbon precursor for SnO_2@carbon core−shell particles. We also demonstrate their promising application as anode materials for lithium-ion batteries. Consistent with the aforementioned hypothesis, the as-prepared carbon-coated SnO_2 nanocolloids exhibit significantly improved cycling performance compared to previously reported SnO_2-based anodes.

Experimental Section

Materials Preparation. Uniform-sized carbon-coated SnO_2 nanocolloids are synthesized in large scale by a simple hydrothermal method followed by carbonization under inert atmosphere. In a typical synthesis, 1.0 g of potassium stannate trihydrate ($K_2SnO_3 \cdot 3H_2O$, Aldrich, 99.9%) was dissolved in 20 mL of 0.8 M (concentrations in the range of 0.2−1.0 M were investigated) aqueous glucose solution. Afterward, the solution was transferred to a Teflon-lined stainless steel autoclave (40 mL in volume), and hydrothermally treated in an air-flow electric oven at 180 °C (temperatures in the range of 160 − 200 °C were investigated) for 4 h. After cooling down naturally, the dark-gray precipitate was harvested by centrifugation and washed thoroughly with ethanol and deionized water. After the mixture was vacuum-dried at room temperature, about 0.75 g of brown-gray powder was obtained. For carbonization, a certain amount of as-obtained powder was loaded into a tube furnace and heated under high-purity N_2 at 450 °C (temperatures in the range of 450 − 700 °C were investigated) for 4 h with a temperature ramp of 4 °C/min. For reduction with H_2, a mixed H_2/N_2 (6% H_2) gas flow was used instead of pure N_2 gas. To burn off the carbon material, the brown-gray powder was calcined in air at 350−500 °C for 1 h.

Materials Charaterization. Products were thoroughly characterized with X-ray powder diffraction (XRD; Scintag PAD X, Cu Kα, λ = 1.5406 Å), field-emission scanning electron microscopy (FESEM; Hitachi S4500), transmission electron microscopy (TEM; JEOL-1200EX, 120 kV). The thermogravimetric analysis (TGA) was carried out under an air flow of 60 mL/min using TA Instruments Q500 from room temperature to 550 °C with a heating rate of 3 °C/min.

Electrochemical Measurement. The electrochemical measurements were carried out using homemade two-electrode Swagelok-type cells with lithium metal as the counter and reference electrodes at room temperature. The working electrode consisted of 80 wt % of the active material (e.g., SnO_2@C), 10 wt % of conductivity agent (carbon black, Super−P-Li), and 10 wt % binder (polyvinylidene difluoride, PVDF, Aldrich). The active material loading in each electrode disk (about 13 mm in diameter) was typically 1−2 mg. The electrolyte was 1 M $LiPF_6$ in a 50:50 w/w mixture of ethylene carbonate and diethyl carbonate. Cell assembly was carried out in a Ar-filled glovebox with the concentrations of moisture and oxygen below 1 ppm. Charge−discharge cycles of the half-cells were measured between 5 mV and 2.0 V (or 3.0 V) at a constant current density with a Maccor 4304 battery tester.

Results and Discussion

Uniform-sized carbon-coated SnO_2 nanocolloids are synthesized in large scale using inexpensive stannate and glucose as precursors. The synthesis is based on a simple hydrothermal method followed by carbonization under an inert atmosphere. Figure 1a displays as-synthesized SnO_2 nanocolloids coated with a thin layer of GCP under

(23) Park, M. S.; Kang, Y. M.; Wang, G. X.; Doti, S. X.; Liu, H. K. *Adv. Funct. Mater.* **2008**, *18*, 455.
(24) Demir-Cakan, R.; Hu, Y. S.; Antonietti, M.; Maier, J.; Titirici, M. M. *Chem. Mater.* **2008**, *20*, 1227.
(25) Larcher, D.; Beattie, S.; Morcrette, M.; Edstroem, K.; Jumas, J. C.; Tarascon, J. M. *J. Mater. Chem.* **2007**, *17*, 3759.
(26) Noh, M.; Kwon, Y.; Lee, H.; Cho, J.; Kim, Y.; Kim, M. G. *Chem. Mater.* **2005**, *17*, 1926.
(27) Wang, Y.; Zeng, H. C.; Lee, J. Y. *Adv. Mater.* **2006**, *18*, 645.
(28) Hu, Y. S.; Demir-Cakan, R.; Titirici, M. M.; Muller, J. O.; Schlogl, R.; Antonietti, M.; Maier, J. *Angew. Chem., Int. Ed.* **2008**, *47*, 1645.
(29) Lou, X. W.; Li, C. M.; Archer, L. A. Adv. Mater. 2009, in press.
(30) Lou, X. W.; Deng, D.; Lee, J. Y.; Archer, L. A. *Chem. Mater.* **2008**, *20*, 6562.
(31) Tarascon, J. M.; Armand, M. *Nature* **2001**, *414*, 359.

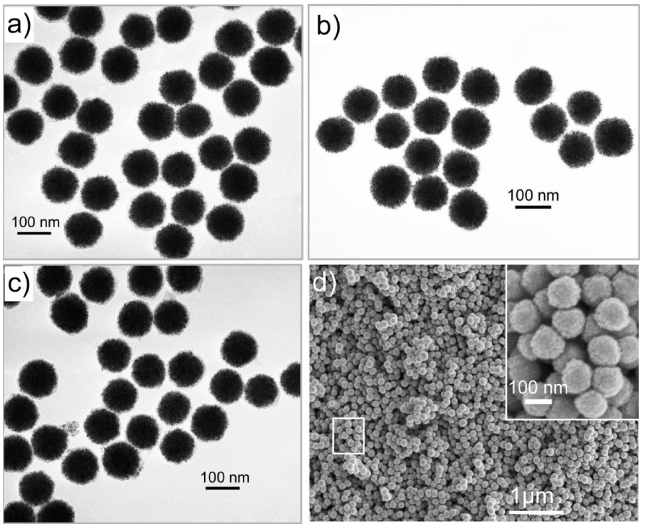

Figure 1. (a) As-synthesized SnO_2 nanocolloids coated with a thin layer of glucose-derived, carbon-rich polysaccharide (180 °C, 0.8 M glucose). (b) As-synthesized SnO_2 colloids with no coating of carbon materials observed (160 °C, 0.8 M glucose). (c, d) Carbon-coated SnO_2 nanocolloids obtained after carbonization of particles shown in a at 450 °C; inset in d is a magnified FESEM image from the area indicated by rectangle.

hydrothermal conditions at 180 °C. As can be seen, these discrete core−shell nanocolloids are nearly monodisperse with a diameter of about 100 nm. Each individual SnO_2 colloid is composed of numerous fine nanoparticles. Although synthesized by a one-pot process, such core−shell nanocolloids are formed by hydrolysis of stannate and subsequent deposition of GCP because of the difference in kinetics. Indeed, our result indicates that SnO_2 nanocolloids synthesized at 160 °C do not have notable GCP coating as shown in Figure 1b. Hydrothermal carbonization of carbohydrates in the temperature range of 160−200 °C has been employed as a facile route for preparation of carbon-rich colloids and coating of carbon-rich materials on various nanostructures by different groups.[26,28,32,33] Formation of GCP under hydrothermal conditions is a complex chemical process with moderate kinetics. From our experience, in general, it is quite challenging to obtain uniform GCP coating on presynthesized nanostructures while minimizing the fraction of GCP spheres in the product.[29,30]

SnO_2 nanospheres can hardly precipitate in a water solution of stannate even in the presence of urea (0.1−1.0 M), which is consistent with our previous systematic investigation on hydrolysis of stannate in a water/ethanol mixed solution.[11] Therefore, it appears that the formation of SnO_2 nanospheres in present protocol is apparently mediated by the mild acidic condition created as a result of hydrothermal treatment of glucose.[34] To verify the important role played by glucose, we investigated the effect of glucose concentration in the range of 0.2−1.0 M on precipitation of SnO_2 nanocolloids and GCP coating while keeping other conditions identical. With a glucose concentration of 0.2 M, only small nanoparticles (gel-like) are

(32) Sun, X. M.; Li, Y. D. *Angew. Chem., Int. Ed.* **2004**, *43*, 597.
(33) Sun, X. M.; Liu, J. F.; Li, Y. D. *Chem. Mater.* **2006**, *18*, 3486.
(34) Ikeda, S.; Tachi, K.; Ng, Y. H.; Ikoma, Y.; Sakata, T.; Mori, H.; Harada, T.; Matsumura, M. *Chem. Mater.* **2007**, *19*, 4335.

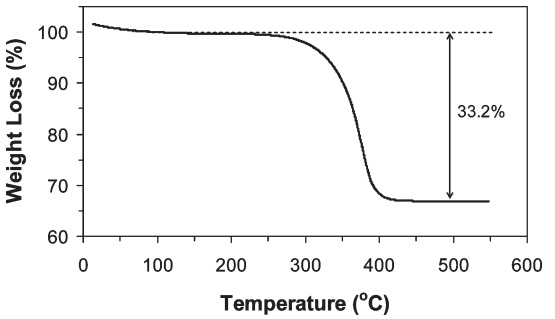

Figure 2. TGA curve of carbon-coated SnO_2 nanocolloids shown in c and d in Figure 1. The weight is normalized at 100 °C since the weight loss below 100 °C is mainly caused by water evaporation.

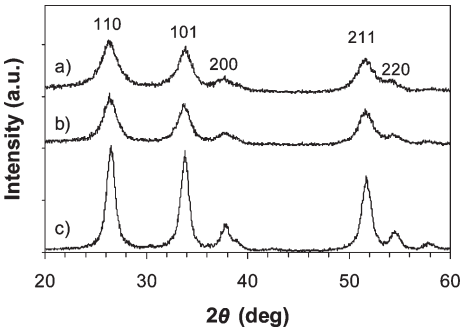

Figure 3. XRD patterns: (a) as-synthesized SnO_2 nanocolloids coated with carbon-rich material (180 °C, 0.8 M glucose); (b) after carbonization at 450 °C; (c) after calcination in air at 500 °C for 1 h.

formed with very low yield even after prolonged hydrothermal treatment (16 h). When the glucose concentration is increased to 0.5 M, the product consists of small nanoparticles and nanospheres with a broad size distribution and moderate yield. Monodisperse SnO_2@GCP nanocolloids (see Figure 1a) are obtained with nearly perfect yield only if the glucose concentration is about 0.8 M.

It has also been known that such GCP can be carbonized at a temperature as low as 400 °C.[30,33] Figure 1 c and d show carbon-coated SnO_2 nanocolloids obtained by carbonizing the as-synthesized SnO_2@GCP nanocolloids at 450 °C. As can be seen, the morphology is largely unaltered. The carbon content in these carbon-coated SnO_2 nanocolloids can be readily determined by thermogravimetric analysis (TGA). As shown in Figure 2, the combustion of carbon begins around 260 °C, and is nearly complete around 400 °C. This temperature is far too low for carbothermal reduction of SnO_2 as will be discussed shortly, and the weight loss below 100 °C is generally attributed to evaporation of adsorbed water. Therefore, the carbon content is directly read from the TGA curve to be about 33.2 wt %.

The crystallographic structure of all samples is characterized by X-ray powder diffraction (XRD). From the XRD pattern (Figure 3a) of the as-synthesized core−shell nanocolloids, the poorly crystalline phase is assigned to tetragonal rutile SnO_2 (JCPDS card no. 41−1445, space group: $P4_2/mnm$, $a_o = 4.738$ Å, $c_o = 3.187$ Å), while noting that GCP is amorphous. The mean crystallite size is estimated to be about 4 nm only using Scherrer's formula based on the (110) peak.[11] According to previous reports, carbothermal reduction of SnO_2 becomes substantial only

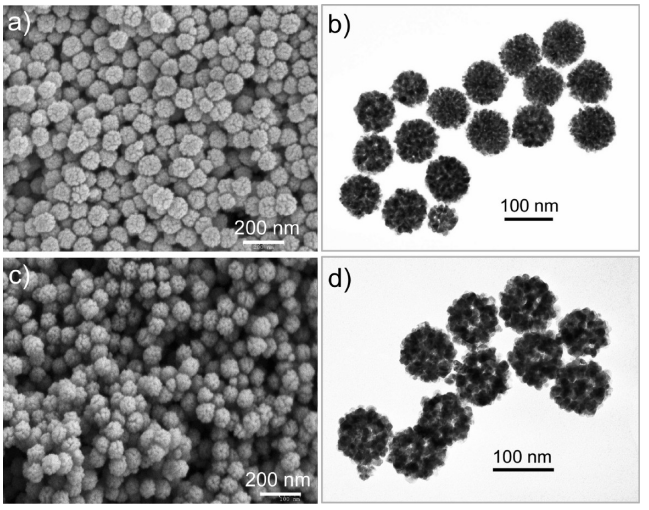

Figure 4. FESEM (a, c) and TEM (b, d) images of SnO_2 nanocolloids obtained after calcination in air at (a, b) 400 °C and (c, d) 500 °C.

when the carbonization temperature reaches around 600 °C.[29,30,33] XRD analysis (Figure 3b) confirms that carbothermal reduction of SnO_2 does not take place during carbonization at 450 °C. Interestingly, the crystallinity of SnO_2 is almost unchanged with the mean crystallite size increased slightly to about 5 nm (from Scherrer's formula). Pure SnO_2 nanocolloids can be obtained by calcining as-synthesized SnO_2@GCP core−shell nanospheres in air. From the XRD pattern shown in Figure 3c, it is observed that the crystallinity of SnO_2 is significantly improved with a mean crystallite size of 9 nm (from Scherrer's formula). Figure 4 shows the resulting SnO_2 nanocolloids after calcination at 400 and 500 °C. Clearly, the nanospherical morphology can be maintained, and as expected, the crystallite size increases with higher calcination temperature (Figure 4, compare d with b), leading to a more porous structure.

We have investigated the lithium storage properties using a normal two-electrode cell, in which lithium foil serves as both counter and reference electrodes. Figure 5a shows a typical discharge−charge voltage profile of carbon-coated SnO_2 nanocolloids for the first cycle at a current density of 120 mA/g. The discharge and charge capacities are observed to be 1337.1 and 948.8 mA h/g, respectively, indicating an irreversible loss of 29%. This irreversible loss should be considered very small for SnO_2-based materials. To further understand this irreversible loss, cyclic voltammetry (CV) measurement was carried out with the result shown in Figure 5b. In good agreement with previous reports,[24,35] two well-defined cathodic peaks are observed in the first cycle. The peak at 0.66 V corresponds to the reductive transformation of SnO_2 to Sn and Li_2O as described by reaction (1), whereas the peak at 0.07 V can be attributed to formation of Li_xSn alloy as described by reaction (2) and insertion of Li into the carbon materials. Interestingly, a trivial peak at 1.68 V is also observed, which cannot be fully understood. Two corresponding anodic

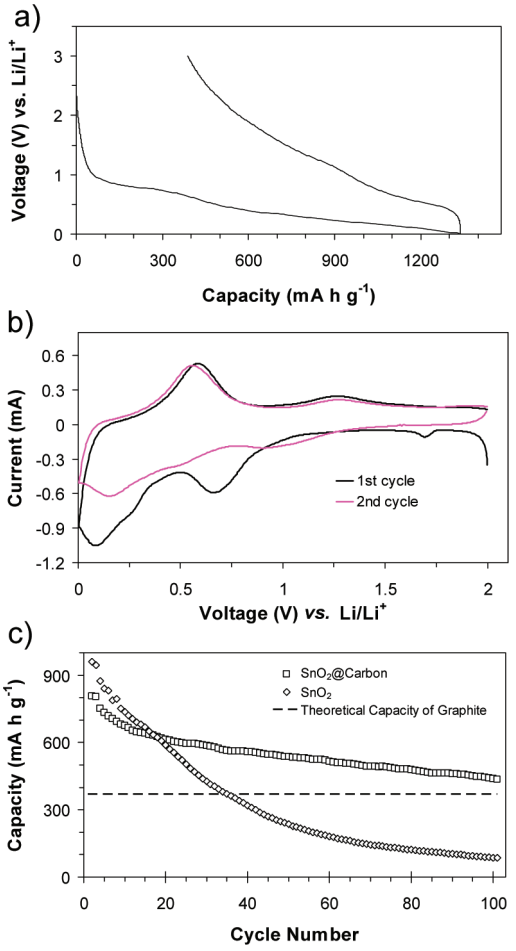

Figure 5. (a) First-cycle discharge−charge voltage profile of carbon-coated SnO_2 nanocolloids shown in Figure 1c at a current density of 120 mA/g. During initial discharge, the cell potential drops rapidly from the open circuit potential of about 3.2 V. (b) Cyclic voltammograms for the first and second cycles between 2 V and 5 mV at a scan rate of 0.1 mV/s. (c) discharge capacities (lithium insertion) vs cycle number between 2 V and 5 mV, the current densities used for SnO_2@carbon and SnO_2 (see Figure 4d) are 300 and 400 mA/g, respectively, by taking the carbon mass of SnO_2@carbon into account.

peaks are observed. One is at about 0.6 V, which indicates dealloying of Li_xSn alloy. The other peak is at about 1.28 V, which might indicate partial reversibility of reaction (1).[24] In the second cycle, both cathodic peaks shift to higher voltages (about 0.14 and 1.0 V), and the peak current reduces substantially. This observation indicates occurrence of irreversible processes during the first cathodic sweep. Apart from the largely irreversible reaction (1), irreversible decomposition of electrolyte could occur at low voltages (for example, formation of solid electrolyte interface, SEI). Because of this, even the carbon material by itself has a huge irreversible loss for the first cycle (see the Supporting Information). However, there is no noticeable current change at both anodic peaks, suggesting that the alloying/dealloying reaction between Sn and Li takes place to the same extent, in other words, it is highly reversible (If this is not true, one should observe significant reduction in anodic peaks during second cycle. Strictly speaking, one should conclude reversibility from cathodic and anodic peaks in the same cycle. However, here the cathodic peak is not well-defined especially in the presence of large fraction

(35) Wen, Z. H.; Wang, Q.; Zhang, Q.; Li, J. H. *Adv. Funct. Mater.* **2007**, *17*, 2772.

of carbon materials), and reaction (1) is reversible to a certain extent. Figure 5c shows the cycling performance of these carbon-coated SnO_2 nanocolloids. It can be observed that the capacity retention is significantly improved compared to cycling performance of previous SnO_2-based materials.[11,18,23,35] Specifically, although the capacity still decays gradually over cycling, a high capacity of 440 mA h/g can be retained after 100 cycles at a current density of 300 mA/g. This performance, although not perfect, is very encouraging, especially in view of the ease in material synthesis. One should also take into account the fact that the composite material contains about one-third of low-capacity carbon (see the Supporting Information). For comparison, the cycling performance of SnO_2 nanospheres obtained by calcination at 500 °C is also provided in Figure 5c. Consistent with previous reports,[11,18,23] the capacity of SnO_2 nanospheres fades quickly to a value below the theoretical capacity of graphite (372 mA h/g) in less than 40 cycles, and to 87 mA h/g only after 100 cycles. The above results clearly indicate the positive impact of carbon nanocoating on capacity retention over extended cycling. Furthermore, it is interesting to observe that the capacity of the SnO_2@carbon material is comparable to that of pure SnO_2 sample in the course of first several cycles despite that the SnO_2@carbon material contains about 33.2 wt % carbon, which has a low capacity of about 200 mA h/g (see the Supporting Information).[30] Therefore, in both samples, the actual capacity of SnO_2 is clearly much higher than the theoretical capacity (790 mA h/g) calculated assuming that only reaction (2) is reversible. Consistent with the above CV result, this observation could suggest that reaction (1) is partially reversible.[24]

When the glucose concentration is further increased to 1.0 M, the GCP coating becomes more predominant, i.e., the particles are largely interconnected by the thick GCP coating. Shown in Figure 6 (a and b) are particles synthesized with a glucose concentration of 1.0 M and carbonized at 550 °C. As can be seen from Figure 6a, the SnO_2 nanospheres are completely embedded in thick carbon shells. From the corresponding XRD analysis (Figure 7b), carbothermal reduction took place to some small extent as suggested by the emerging small peaks (compared to Figure 7a) which can be assigned to SnO and Sn. When carbonization was carried out at 700 °C, XRD analysis revealed that SnO_2 was completely reduced to metallic Sn, which because of its very low melting point (232 °C) evaporated to form big beads in micrometer or even millimeter size. As a result, abundant carbon hollow nanospheres were produced as shown in Figure 6c. For this reason, carbon-coated Sn nanospheres can hardly be prepared by carbothermal reduction of SnO_2. We therefore explored another approach. Specifically, we included a small fraction of H_2 gas to reduce SnO_2 during carbonization, which was carried out at a lower temperature of 550 °C. At this temperature, evaporation of Sn is insignificant. Confirmed by XRD analysis (Figure 7c), polycrystalline SnO_2 was completely reduced to metallic β-Sn (JCPDS card no. 04−0673). From the TEM image shown in Figure 6d, the as-formed Sn nanospheres are still confined

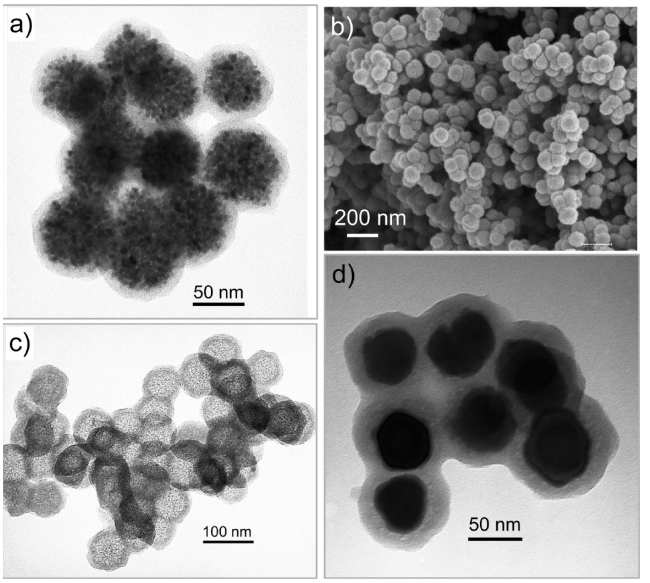

Figure 6. (a, b) Carbon-coated SnO_2/Sn nanospheres obtained after carbonization at 550 °C. (c) Carbon hollow nanospheres obtained after carbonization at 700 °C. (d) Carbon-coated Sn nanospheres obtained after H_2 reduction at 550 °C. The SnO_2/polysaccharide nanospheres were synthesized at 180 °C with a glucose concentration of 1.0 M.

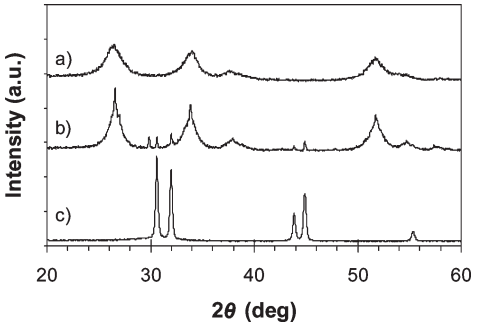

Figure 7. XRD patterns: (a) as-synthesized SnO_2/polysaccharide nanospheres (180 °C, 1.0 M glucose); (b) after carbonization at 550 °C; (c) after H_2 reduction at 550 °C.

inside the carbon shells. Because of significant shrinkage of GCP during carbonization, it appears that the Sn nanospheres are tightly wrapped by the carbon shells.[29] Again, the carbon content in both SnO_2@carbon and Sn@carbon samples can be determined by TGA. From the TGA curve (Figure 8a), it can be directly observed that there is about 51.9% of carbon in the SnO_2@carbon sample since the Sn content is insignificant as suggested by XRD analysis above. For the TGA curve of Sn@carbon (Figure 8b), the initial weight gain in the temperature range of 210−330 °C is due to oxidation of Sn by O_2 forming SnO_2. From the overall weight loss of 45.9%, the carbon content of Sn@carbon can be calculated to be 57.4%, which is in good agreement with 51.9% of carbon in corresponding SnO_2@carbon.

It has been argued that one major drawback of SnO_2-based anode materials is their initial large irreversible loss of lithium, which is generally ascribed to the irreversible reduction of SnO_2 to Sn (reaction 1) in the field.[23,35] If this indeed is the cause, use of Sn-based anodes should be advantageous. The two samples (SnO_2@carbon vs Sn@carbon) obtained above possess similar structure,

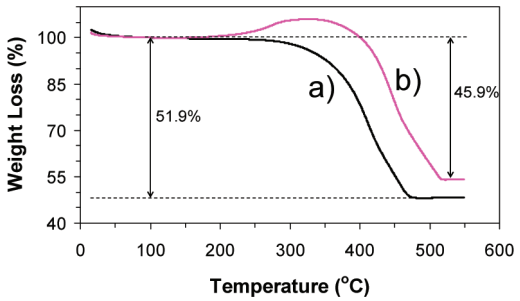

Figure 8. TGA curves: (a) carbon-coated SnO_2/Sn nanospheres shown in Figure 6a; (b) carbon-coated Sn nanospheres shown in Figure 6d. The weight is normalized at 100 °C because the weight loss below 100 °C is mainly caused by water evaporation.

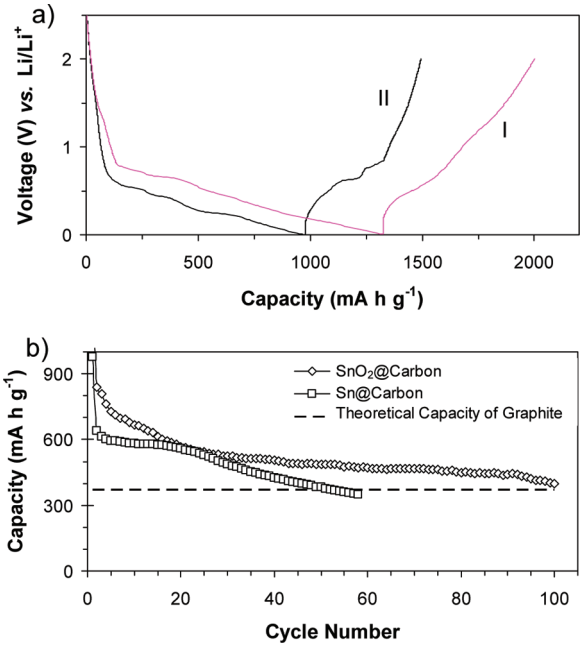

Figure 9. (a) First-cycle discharge−charge voltage profiles for SnO_2@-carbon (I, see Figure 6a) and Sn@carbon (II, see Figure 6d). (b) Discharge capacities (lithium storage) vs cycle number between 2 V and 5 mV at the same current density of 120 mA/g.

morphology and size. We thus investigated their comparative lithium storage properties. Figure 9a shows the first-cycle discharge−charge voltage profiles for both samples. Despite the large difference in the first-discharge capacity (1325 vs 979 mA h/g), it is surprisingly found that both samples have similar initial irreversible loss after charging to 2 V, namely, 49 vs 48% for SnO_2@carbon and Sn@carbon, respectively. Similar large irreversible loss was also observed previously for a Sn−C composite material by Scrosati and co-workers.[36,37] This observation might be explained as follows. On the one hand, for SnO_2@carbon the conversion reaction (1) is at least in part reversible as supported by the CV measurement and also suggested by others,[24,33] probably in a similar mechanism as transition metal oxides.[38] This argument will also help explain a common observation that reversible lithium storage capacity of SnO_2 can often be much higher than the theoretical value of 790 mA h/g based on reaction (2) during the first 10 cycles.[9,11,39] On the other hand, it might be generally concluded that the large initial irreversible loss could be mainly caused by formation of solid-electrolyte interface (SEI) and decomposition of electrolyte at a low voltage as similarly observed for pure carbon material (see the Supporting Information). It is also interesting to note that catalytic decomposition of electrolyte by pure Sn crystallites might be responsible for an anomalous high-voltage (> 1.0 V) irreversible capacity in Sn electrodes.[40] But this possibility can be clearly ruled out in the present work because the capacity contribution above 1.0 V is insignificant. Figure 9b shows the comparative cycling performance. The initial total capacity of Sn@carbon (around 560−600 mA h/g) is generally consistent with the additive contributions by weight fraction from Sn (about 430 mA h/g) and carbon matrix (about 160 mA h/g). The capacity of Sn@carbon fades gradually to about 560 mA h/g after 20 cycles and then quickly to a value below 372 mA h/g after 52 cycles. This might be understood in view of the structural features of these Sn@carbon nanospheres (see Figure 6d). Specifically, the confined Sn nanospheres of 50−80 nm in size are probably too large, and in addition it appears no interior hollow space for accommodating the large volume change during discharging-charging cycles.[11,22,36,41,42] In contrast, each carbon-coated porous SnO_2 nanosphere is composed of numerous small crystallites (see Figure 6a). As a result, the SnO_2@carbon nanospheres can deliver a capacity higher than the theoretical capacity of graphite (372 mA h/g) for 100 cycles.

Conclusions

In summary, nearly monodisperse carbon-coated SnO_2 nanocolloids have been synthesized in gram scale by a simple hydrothermal method followed by carbonization. When tested for reversible lithium storage, these SnO_2@-carbon core−shell nanocolloids manifest significantly improved cycling performance compared to SnO_2 nanospheres. A high capacity of 440 mA h/g can be retained after 100 cycles. Our result clearly demonstrates that carbon nanocoating can be an effective way for improving cycling performance of noncarbonaceous anode materials for lithium ion batteries. Carbon-coated Sn nanospheres can also be obtained by reduction of SnO_2 with H_2 at a relatively low temperature. Our comparative study suggests that the large initial irreversible loss is mainly caused by formation of solid-electrolyte interface (SEI) and decomposition of electrolyte. Given the synthetic ease, scalability for mass production, and excellent lithium storage properties, we believe these SnO_2 nanocolloids

(36) Derrien, G.; Hassoun, J.; Panero, S.; Scrosati, B. *Adv. Mater.* **2007**, *19*, 2336.
(37) Hassoun, J.; Derrien, G.; Panero, S.; Scrosati, B. *Adv. Mater.* **2008**, *20*, 3169.
(38) Poizot, P.; Laruelle, S.; Grugeon, S.; Dupont, L.; Tarascon, J. M. *Nature* **2000**, *407*, 496.
(39) Deng, D.; Lee, J. Y. *Chem. Mater.* **2008**, *20*, 1841.
(40) Beattie, S. D.; Hatchard, T.; Bonakdarpour, A.; Hewitt, K. C.; Dahn, J. R. *J. Electrochem. Soc.* **2003**, *150*, A701.
(41) Lee, K. T.; Jung, Y. S.; Oh, S. M. *J. Am. Chem. Soc.* **2003**, *125*, 5652.
(42) Ma, H.; Cheng, F. Y.; Chen, J.; Zhao, J. Z.; Li, C. S.; Tao, Z. L.; Liang, J. *Adv. Mater.* **2007**, *19*, 4067.

coated with or without carbon would attract wide interest in lithium ion batteries, sensors, and other important applications.

Acknowledgment. The authors are grateful to the National Science Foundation (DMR0404278) and for Award KUS-C1-018-02 made by King Abdullah University of Science and Technology (KAUST) for partial support of this study. Facilities available through the Cornell Center for Materials Research (CCMR) and Cornell Integrated Microscopy Center (CIMC) were also used in this work.

Supporting Information Available: SEM image, charge−discharge curves, and cycling performance of carbon nanospheres (PDF). This information is available free of charge via the Internet at http://pubs.acs.org.